Simplification, Conservation and Adaptivity in the Front Tracking Method

E. George[1], J. Glimm[1,2], J. W. Grove[3], X. L. Li[1], Y. J. Liu[1], Z. L. Xu[1], and N. Zhao[1]

[1] SUNY at Stony Brook, Stony Brook, NY 11794 *linli@ams.sunysb.edu*
[2] Brookhaven National Laboratory, Upton, NY 11973 *glimm@ams.sunysb.edu*
[3] Los Alamos National Laboratory, Los Alamos, NM 87545 *jgrove@lanl.gov*

1 Introduction

The front tracking method was first introduced by Richtmyer for the numerical solution of hyperbolic equations. The solution of hyperbolic equations contains discontinuities such as contact discontinuities and shocks. The former exist even in linear equations when the initial condition is discontinuous. The latter are associated with the nonlinearity of the hyperbolic system. Finite difference and finite volume methods give a satisfactory numerical approximation and convergence rate in the region where the solution is smooth. However they fail to deliver physically correct solutions at discontinuities, especially when the equation of state across the discontinuity is sharply different. By separating the smooth regions at the discontinuity through an interface, the front tracking method overcomes this numerical difficulty by applying finite difference solvers to each smooth subdomain while treating the discontinuity with special care and propagating the front using the exact solution of the Riemann problem.

In the last few years, progress has been made to extend the front tracking method to three dimensional space and to address the issue of conservation in the coupling between the front solution and the interior solver. There has also been an effort to combine tracking and adaptive mesh refinement in the computation of the hyperbolic equations. In this paper, we will review the work done in this field. We will describe the addition of the grid-based tracking and hybrid methods, the use of dynamic flux and control volume for conservative tracking and the combination of the adaptive computational code Overture and the front tracking code FronTier.

A major thrust of the front tracking program has been its application to scientific problems. In this paper, we report on one of the most successful applications of the front tracking method to fluid physics. The clear separation of different fluid components in the computation of gravity driven Rayleigh-Taylor instability has maintained correct buoyancy driven acceleration throughout the numerical simulation, thus giving a dimensionless acceleration consistent with that observed in experiments.

Sections 2, 3, and 4 will discuss recent developments of the front tracking method, its simplification and extension to three dimensional space, implementation of the conservative tracking scheme and the merging of FronTier with the Overture code, while Section 5 will discuss a successful application of the front tracking method. A short conclusion is given in Section 6.

2 Geometrical Simplification

The classical front tracking method in which the front geometry is independent of the rectangular grid of the computational domain has encountered an increased difficulty in its extension to the three dimensional space. The main reason for this fact is: (1) the determination and correction of the interface topology requires the information of the full interface and (2) the interface could evolve into a configuration with high complexity, even within one time step and with small probability. This has limited the robustness of the numerical algorithm and increased the complexity of the code in order to handle cases which may rarely occur (but when they happen, they terminate the computation). Such complexity already occured in two dimensional front tracking, but became a significant obstacle when the front tracking is extended to three dimensions.

To resolve this problem, a new method, called the grid-based tracking method [5], was introduced to augment the classical or the grid-free tracking method. This method makes a closer link between the interface and the rectangular grid of the computational domain. The interface is grouped into segments each fit into a mesh block in the rectangular grid. With an artificially imposed constraint that the interface is allowed to intercept each mesh block edge only once, the topology of the interface within each mesh block is greatly simplified. In two dimensions, there are only three isomorphically distinct cases and in three dimensions, only 14 isomorphically distinct cases. The construction of the block interface is the same as in the marching cube method by Lorensen and Cline [8], but the reconstruction is dynamic. Since the level set method [9] also borrows the marching cube based graphical tools to show the interface, the simplicity as well as the resolution level of the interface is the same for both methods. Figures 1 and 2 show the comparison of the interface in the classical (or grid-free) tracking method and the grid-based tracking method.

While gaining robustness, the grid-based tracking method loses resolution. The quality of its elements is also decreased due to the constraint imposed by the rectangular grid blocks. In two dimension, these interface elements are bonds and in three dimension, they are triangles. To combine the merits of the two tracking method, we also propose a hybrid method. The hybrid algorithm can vary according to the application needs. One method is the failure backing-up algorithm in which the grid based method is used only when the grid-free method fails to resolve the topological changes. In that case, the

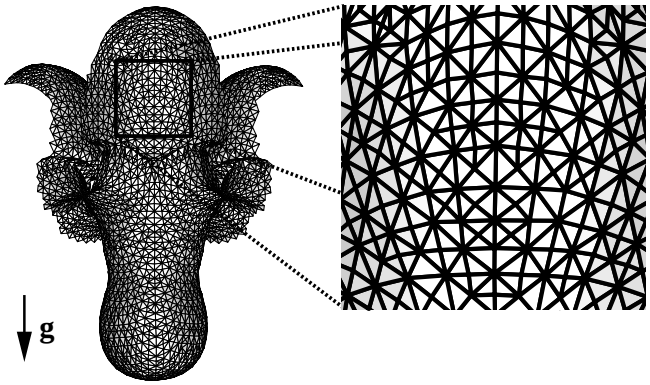

Fig. 1. The the grid-free interface in the simulation of Rayleigh-Taylor instability

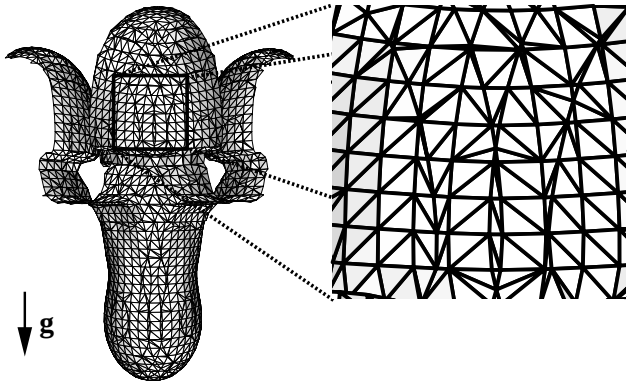

Fig. 2. The reconstruction of the grid-based interface in the simulation of Rayleigh-Taylor instability

whole interface will be reconstructed through the grid-based method. Another one is the locally grid-based method. In such a method when a topological bifurcation is detected, a rectangular box of varying size is constructed which totally confines the region of the interface tangling and only interface pieces inside the box will undergo a grid-based reconstruction.

The grid-based reconstruction of the interface mesh consists of four major steps: (1) the propagation of the interface, (2) intersection of the interface with grid edges, (3) removal of the unphysical or topologically incorrect intersections, and (4) the block-wise reconstruction of the interface. The details of this algorithm are presented in [5]. Figure 3 shows the evolution of a 3-D Rayleigh-Taylor unstable interface in a front tracking simulation.

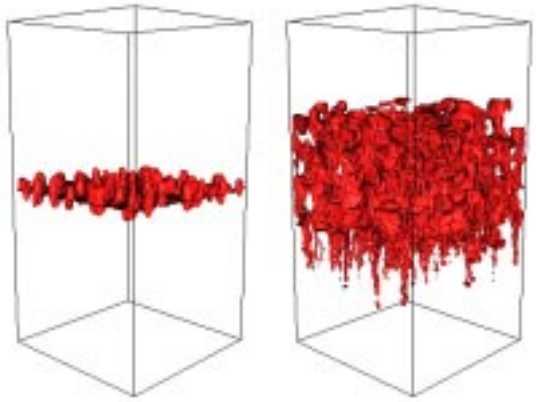

Fig. 3. Evolution of the fluid interface in the simulation of Rayleigh-Taylor instability with randomly perturbed initial interface

3 Conservation

The second important issue we have addressed in the front tracking method as well as in other tracking methods (such as the level set tracking method), is the conservation property of the numerical scheme. To separate different material components and prevent the cross-interface interpolation (such interpolation is the source of numerical diffusion and dispersion), the front tracking method used extrapolated states from the interface to create the numerical stencil to update the near-interface grid points [7]. This algorithm was later adopted to use in the level set tracking and was called the ghost-cell method [3]. For example, to use a five-point MUSCL or a Godunov-type scheme to update the states at two grid points j and $j+1$ between which there is an interface, we calculate the flux at the right cell edge of point j through $F_{j+1/2}(u^n_{j-1}, u^n_j, u^{\bar{n}}_{j+1}, u^{\bar{n}}_{j+2})$, and the flux at the left cell edge of point $j+1$ through $F_{j+1/2}(u^{\bar{n}}_{j-1}, u^n_j, u^n_{j+1}, u^n_{j+2})$, where $u^{\bar{n}}_{j+1}$, $u^{\bar{n}}_{j+2}$ are ghost states extrapolated from the left side of the interface, and $u^{\bar{n}}_{j-1}$,$u^{\bar{n}}_j$ are the ghost states extrapolated from the right side of the interface. Since the two fluxes calculated at the right cell edge of j and the left cell edge of $j+1$ cannot cancel with each other, the numerical scheme is not conservative. The lack of conservation occurs in the same way in the level set tracking, the difference between the two methods lying in the algorithm of extrapolation.

Our new numerical scheme [6] is based on the concept of dynamic flux defined as:

$$f^d_J(u) = f(u_J) - s u_J, \qquad J = L,\ R$$

where $f(u)$ is the stationary flux and s is the front speed. When the dynamic flux is applied at a dynamical cell edge (the interface), with complete sep-

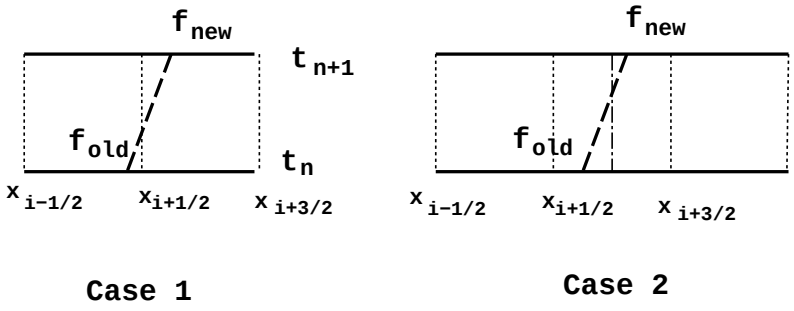

Fig. 4. The 1-D time space cells. The left is without merging and the right is with merging with neighboring cells.

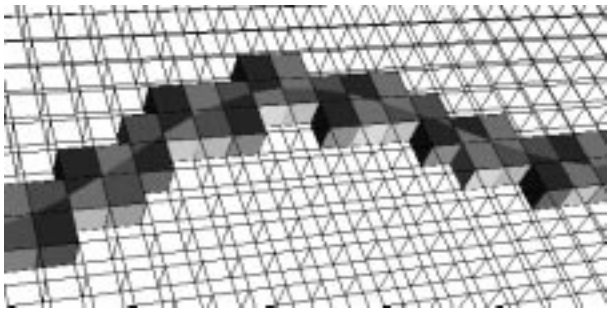

Fig. 5. The 2-D time space cells for the computation of conservative front tracking

aration of fluid states on each side of the interface, we can still have flux cancellation so long as the state variables u_L and u_R are the solution of the Riemann problem and thus satisfy the Rankine-Hugoniot condition. The implementation of the new scheme is based on the construction of the space-time control volume. Figures 4 and 5 show the control volumes for one and two space dimensions.

The conservation law for a control volume with a dynamic boundary can be written as

$$(u_+ - u_-)n_t + \sum_{j=1}^{d}(F_j(u_+) - F(u_-))n_{xj}) = 0$$

where n_t and n_{xj} are the time and space components of the unit vector at the boundary of the space-time control volume. This condition is satisfied at any space-time control volume boundary, should it be discontinuous or not. In particular, we use the space-time interface as one side of the control volume so that cross-interface interpolation can be avoided. The accuracy of the scheme is then dependent on the algorithm to evaluate u_+ and u_- on each side of the control volume.

4 Adaptivity

Front tracking is most effective in separating the fluid components, especially those with different equation of states. Tracking of shock waves is more easily replaced by other methods such as capturing with the use of limiters. The interaction of different waves can be easily solved in one dimension. In two dimensions, although the shock polar solution allows tracking of both contacts and shocks, there are cases in which the 2D required Riemann problem does not have a simple solution. In three dimensions, the problem of wave interactions in gas dynamics is yet to be studied. Another reason for not tracking shocks is that such discontinuities are compressive. With converging characteristics, numerical errors tend to be annihilated at the discontinuity and diffusion is self-adjusted. Capturing methods with the application of limiters provide a satisfactory solution to such nonlinear discontinuities.

Unlike the contact surface which separates materials with different equation of states, a shock wave does not have to be prescribed initially. Even if the initial condition does not contain a shock discontinuity, one can be generated in the interior of the computational domain after a finite time. The resolution required by these localized but captured waves is typically distributed very nonuniformly in space. Adaptive mesh refinement [1] provides a very effective and efficient computational platform to deal with this problem. A combination of the front tracking and adaptive mesh refinement will compliment each other and become a very powerful tool to study problems in fluid physics with both prescribed material boundary and interior wave dynamics.

The adaptive mesh refinement code we use is adopted from the Lawrence Livermore National Laboratory. The algorithm used in this code follows Berger. The concentration of dynamical changes are detected by the gradient of the physical quantities such as the density and pressure. Grid patches at different levels of refinement are created according to the user prescribed input parameters. Since the material interface is always discontinuous and has the largest gradient, it will always be included in patches of the finest level. Therefore we embed the tracked interface only in the most refined level of the adaptive grid. Figure 6 shows the adaptive patches with a tracked front in the finest level of the grid.

5 A Scientific Application

One of the successful applications of the front tracking method is its application to the gravity driven fluid interface instability, the Rayleigh-Taylor instability. Over the last decade, scientists have been trying to reproduce through computation the experiments done by Read and Youngs on the RT instability with randomly perturbed fluid interface. Read and Youngs first

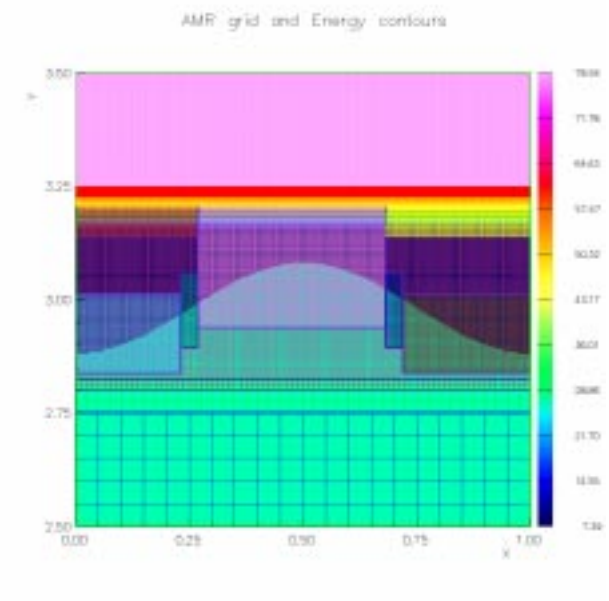

Fig. 6. The adaptively refined patches and the tracked front in a combined Overture-FronTier initialization.

observed that there exists a dimensionless acceleration rate of the mixing layer

$$\alpha = \frac{h}{Agt^2}$$

where h, A, g and t are the height of the mixing layer, the Atwood number of the two fluids, gravity and time respectively. The measurement by Read [10] on the acceleration rate α of the mixing layer on the bubble side gives its values at about $0.06 - 0.077$. However, most of the numerical simulation with untracked fluid interface gives the acceleration rate in the range of $0.015 - 0.04$. The sharp contrast between experiment and computation stimulated intense debate among scientists as to what could be wrong with the experiment or the simulation.

To answer this question, we have performed a comparative study of the RT instability using both an untracked numerical code and the front tracking method. Our front tracking simulation showed an [4] acceleration rate lying within the range of experimental variation. The average value of the α in the front tracking simulation is about 0.07 while the untracked code (using the TVD scheme) gives much smaller acceleration rate of about 0.04, which agrees with most of the simulations by other computational scientists using untracked code. The front tracking value for α has been reanalyzed using lower than leading order asymptotics, yielding a corrected $\alpha = 0.0625$ [2]. A careful study of the fluid density profile revealed a sharp contrast between the

tracked and untracked simulations. The former maintains a clear boundary of the two fluids with a sharp density discontinuity across the fluid interface, while the latter has significant smearing-out of the fluid from one side to the other.

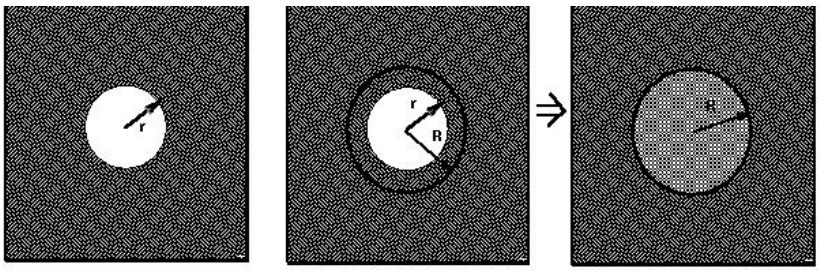

Fig. 7. The buoyancy acceleration for undiffused and diffused bubbles, see text for explanation.

An analysis of the net buoyancy (acceleration) acting on the bubbles (and spikes) revealed that the diffusive layer between the two fluids can significantly retard the relative motion between the two fluids. The reduced mixing rate due to unphysical numerical diffusion can be understood from Figure 7. The left frame represents an immiscible bubble of radius r. The central and the right frame assume that this bubble is smeared out numerically to a radius R while the total mass inside the sphere of radius R is conserved. The buoyancy forces

$$f_1 = f_2 = \frac{4\pi r^3}{3}(\rho_H - \rho_L)g \tag{1}$$

for the bubbles in frames (a) and (c) are the same. However, due to the difference between the mass in the nondiffused bubble (a) and the diffused bubble (c), the two acceleration rates

$$a_1 = \frac{\rho_H - \rho_L}{\rho_L}g \quad > \quad a_2 = \frac{\rho_H - \rho_L}{\rho_L + \left(\frac{R^3}{r^3} - 1\right)\rho_H}g \tag{2}$$

are different. In the diffused fluids, the buoyancy force is distributed to a larger amount of mass, thus reducing the acceleration of the bubble.

We then computed an effective Atwood number $A(t)$ as a function of time for the untracked simulations. This is determined from the highest and lowest densities in a horizontal slice, with the resulting time and space dependent Atwood number averaged over heights in the upper third of the mixing zone at a fixed time to get an Atwood number dependent on time alone. The time dependence of $A(t)$ in the *FronTier* simulation is caused purely by (small)

compressibility effects. For the mass diffusive TVD simulation, the initial density contrast, $A(t=0)=0.5$, is almost completely washed out; the earliest time displayed shows $A(t=2)\approx 0.15$. As new pure (heavy and light) fluid is injected into the mixing region, the effective Atwood number increases, but it is still reduced to about $A\approx 0.3$ on a time averaged basis, or nearly a 50% reduction relative to its initial value.

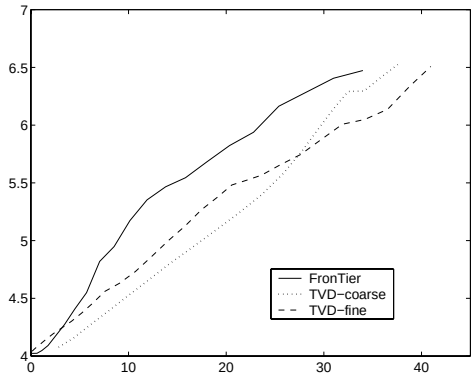

Fig. 8. Bubble height vs. $A_{eff}gt^2$ in tracked and untracked numerical simulation

To compensate for the time dependent Atwood number $A(t)$, we define an effective alpha, $\alpha_{\text{eff}} \approx h/2\int\int A(s)gdsdt$. Specifically, α or α_{eff} is defined here as the slope of the straight line joining the beginning and end of the $h(t)$ curve in Figure 8. This definition, although somewhat arbitrary, is conventional, and thus allows comparison to the results of others. We observe an improved comparison between *FronTier* and TVD and between TVD and experiment. On this basis, we can state that the diffusive buoyancy renormalization of α is capable of resolving existing discrepancies among simulations, among diffusive and non-diffusive simulations and with theory.

6 Conclusion

We conclude that front tracking method can overcome its complexity in handling the interface geometry with the help of the rectangular grid. Using the grid edges as the basis for the interface, we can reduce most of the geometrical calculation to a single coordinate and limit the topological configuration of the interface to small number of isomorphically distinct cases. While combining with the classical grid-free tracking, we can also have the flexibility of enhancing the quality of the interface meshing and maintaining higher resolution of the interface for certain physical problems.

Conservation of the front tracking method can be achieved through construction of space-time control volumes and application of the dynamic flux

at its moving boundary. In combining the front tracking method and the adaptive mesh refinement, we will create a powerful tool for the solution of hyperbolic conservation laws with contact surfaces separating different materials and efficiently resolve the internal wave interactions.

Front tracking method is shown to be able to deliver solutions with sharp contrast to the untracked numerical methods in comparison with experiments. The prediction of the correct acceleration rate in the simulation of RT instability with randomly perturbed interface provides a good example of its success.

7 Acknowledgements

The authors of this work were supported in part by the grants from DOE DEFC0201ER25461, DEFG0398DP00206, DEFG0290ER25084, the grant by the Army Research Office DAAD190110642, and the contract from Los Alamos National Laboratory 26730001014L.

References

1. M. Berger and P. Colella, *Local adaptive mesh refinement for shock hydrodynamics*, J. Comp. Phys., 82 (1989), pp. 64–84.
2. B. Cheng, J. Glimm, and D. H. Sharp, *Dynamical evolution of the Rayleigh-Taylor and Richtmyer-Meshkov mixing fronts*, Submitted to: Phys. Rev. E, (2001). SUNYSB-AMS-01-07 State Univ. of New York at Stony Brook.
3. R. P. Fedkiw, T. Aslam, B. Merriman, and S. Osher, *A non-oscillatory Eulerian approach to interfaces in multimaterial flows (the ghost fluid method)*, J. Comp. Phys., 152 (1999), pp. 457–492.
4. E. George, J. Glimm, X. L. Li, A. Marchese, and Z. L. Xu, *A comparison of experimental, theoretical, and numerical simulation Rayleigh-Taylor mixing rates*, Proc. National Academy of Sci., 99 (2002), pp. 2587–2592.
5. J. Glimm, J. W. Grove, X.-L. Li, and D. C. Tan, *Robust computational algorithms for dynamic interface tracking in three dimensions*, SIAM J. Sci. Comp., 21 (2000), pp. 2240–2256.
6. J. Glimm, X.-L. Li, and Y.-J. Liu, *Conservative front tracking in one space dimension*, Contemporary Mathematics, (2002). Proceedings of the Joint Summer Research Conference on Fluid Flow and Transport in Porous Media: Mathematical and Numerical Treatment. In Press, Report SUNYSB-AMS-01-16.
7. J. Glimm, D. Marchesin, and O. McBryan, *A numerical method for two phase flow with an unstable interface*, J. Comp. Phys., 39 (1981), pp. 179–200.
8. W. E. Lorensen and H. E. Cline, *Marching cubes: A high resolution 3D surface construction algorithm*, Computer Graphics, 21 (1987), pp. 163–169.
9. S. Osher and J. Sethian, *Fronts propagating with curvature-dependent speed: Algorithms based on Hamilton-Jacobi equations*, Jour. Comp. Phys, 79 (1988), pp. 12–49.
10. K. I. Read, *Experimental investigation of turbulent mixing by Rayleigh-Taylor instability*, Physica D, 12 (1984), pp. 45–58.